INDEX COPERNICUS INTERNATIONAL

Bio-Algorithms and Med-Systems

WWW.BAMSJOURNAL.COM ISSN: 1896-530X

ORIGINAL ARTICLE

Received: 13.11.2023
Accepted: 04.12.2023
Published: 31.12.2023

CITE THIS ARTICLE AS:
Konieczka P, Raczynski L, Wislicki W, "Convolutional neural networks in the classification of multiphoton coincidences in a J-PET scanner", Bio-Algorithms and Med-Systems vol. 19, no. 1, pp. 43-47, 2023, DOI: 10.5604/01.3001.0054.1823

AUTHORS' CONTRIBUTION:
A – Study Design
B – Data Collection
C – Statistical Analysis
D – Data Interpretation
E – Manuscript Preparation
F – Literature Search
G – Funds Collection

CORRESPONDING AUTHOR:
Paweł Konieczka MSc; Department of Complex Systems, National Centre for Nuclear Research, Otwock-Świerk, Poland; Andrzej Sołtana St. 7, 05-400 Otwock-Świerk, Poland; E-mail: pawel.konieczka@ncbj.gov.pl

Convolutional neural networks in the classification of multiphoton coincidences in a J-PET scanner

Paweł Konieczka[BE], Lech Raczyński[ADEF] (ORCID: 0000-0002-7039-2084), Wojciech Wiślicki[ADEG] (ORCID: 0000-0001-5765-6308)

Department of Complex Systems, National Centre for Nuclear Research, Otwock-Świerk, Poland

ABSTRACT

This work describes an investigation into the utilization of convolutional neural networks for the classification of three-photon coincidences, focusing specifically on the para--positronium decay associated with a photon from nuclear deexcitation. The data were simulated using the Monte Carlo method, with scandium-44 as the source of β^+ decays. A preprocessing method that allowed for initial cleaning of the training data was described. Subsequently, the parameters of the method for transforming tabular data into images were optimized. Finally, the created images were used to train a binary classifier using a convolutional network model. The developed data preprocessing step and transformation method into image format enabled the achievement of a precision rate of 52% at a sensitivity level of 95%, which was a 10 percentage point improvement compared to the logistic regression model.

KEYWORDS

positron emission tomography, convolutional neural network, positronium, J-PET, para-positronium

INTRODUCTION

Studies on positron emission tomography (PET) involve determining the spatial distribution of a selected substance's concentration in a body, in some cases also its time evolution [1, 2]. To accomplish this, a radiopharmaceutical is administered to the patient. In the basic measurement scheme, information about the electron-positron annihilation events is collected in the form of a line that connects the detected locations and passes through the point of annihilation. This line is referred to as the line of response (LOR). The collection of registered LORs serves as the foundation for PET image reconstruction.

Para-positronium (p-Ps), a short-lived, unstable, spinless atom composed of an electron and a positron [3], can be employed in PET imaging, facilitating more precise localization of annihilation sites by

incorporating information about a third, so called "prompt photon" coming from nuclear deexcitation [4, 5]. In its conventional configuration, PET instrumentation detects coincident pairs of 511 keV annihilation photons, a strategy that indeed offers exquisite spatial resolution but inherently limits the precision of signal localization. The use of a β^+-radioactive isotope, however, gives an opportunity to capitalize on the prompt photon emitted from its decay process, introducing a third photon into the detection schema.

The first approach in converting nonimage data into an image format for CNN architectures was introduced in [6]. A method known as DeepInsight was employed, which involved the construction of an image by grouping similar elements of 1-D input vectors together and separating dissimilar ones, thereby facilitating the collective utilization of neighbouring elements. Those 2-D images were further processed by a CNN model. This concept was further refined and implemented in a previous work [7]. In addition, featured engineering was incorporated, enabling the efficient analysis of data with a limited number of features.

In this study a data transformation into images was employed. These images were subsequently utilized for binary three--photon coincidence classification through the application of a convolutional neural network. We investigated the quality of the proposed approach by considering the problem of three-photon coincidence event classification in the Jagiellonian PET (J-PET) scanner [5, 8–11].

Geant4 SIMULATION SETUP

A Monte Carlo simulation was conducted using a specialized Geant4 Application for Tomographic Emission (GATE) open-source software [12, 13]. A ^{44}Sc isotope was used as a source of β+ decay via the following reaction: $^{44}\mathrm{Sc} \rightarrow {}^{44}\mathrm{C}\alpha^* + \nu \rightarrow {}^{44}\mathrm{C}\alpha + \gamma + e^+ + \nu$, where γ has 1157 keV.

The J-PET scanner geometry was implemented in GATE. The 2-layer detector was composed of seven rings, with each ring being composed of 24 cylindrically arranged modules. Each module was constructed from 32 plastic scintillator strips (16 strips per layer), with a width of 30 mm and a length of 330 mm. The gap length between adjoining rings was 20 mm, and the detector was a cylinder with a radius of 415 mm. The simulation setup was kept consistent with the one utilized in our previous works [7, 14, 15]. The investigated source of radiation was the NEMA IEC phantom [16].

PREPROCESSING STEP

A block diagram (Fig. 1.) shows the preprocessing step for cleaning the data before applying the classification model. A coincidence event was characterized as a sequence of three consecutive photon interactions detected within a specified 3-ns time window. Furthermore, only events meeting the criteria of precisely three interactions, each depositing energy exceeding 200 keV in the detector, were considered valid. Secondly, in each of the selected three-photon coincidences an examination was conducted to determine which photons generated an energy deposition equal to or exceeding 370 keV [17]. Those meeting this criterion were denoted as prompt photon candidates. The threshold for segregating photons into a annihilation and deexcitation group was determined through a data-driven approach using simulated events, aiming to maximize the classification accuracy. The left path in Fig. 1. primarily pertains to instances where multiple photons deposit energies exceeding 370 keV. In this context, it is worth noting that the majority of these coincidences predominantly consist of multi-prompt photons, with only a minuscule fraction, less than a permille, constituting the genuine signal. In contrast, the right path portrays situations in which none of the involved photons exceed an energy of 370 keV, rendering the configuration of these three photons, in a 2 + 1 arrangement, unclear and challenging to discern. The focus of this research is on the middle path, where it is assumed that the highest energy photon comes from deexcitation.

To refine the dataset and exclude events occurring outside the detector's field of view, two selection criteria were applied, analogous to the two-photon experiment [7]. The first criterion required that the reconstructed annihilation point's position in the plane perpendicular to the detector axis be limited to a circular area with a 30-cm radius, while the second constrained the reconstructed position along the axial direction to be within 20 cm of the detector's center.

RESULTS AND DISCUSSION

In contrast to the investigation of two-photon coincidences [7], this study extended its scope by using an additional, prompt photon. The selected features were: the deposited energies of individual photons, the lengths of paths they traveled from the reconstructed emission point to the detector, the attenuation coefficient along the line between two detection points of the annihilation photons, the calculated positronium lifetime, the difference in the detection times of the annihilation photons and the angular difference in the trans-axial section between the detection points of the annihilation photons.

These 10 features were subsequently employed in generating input images for the convolutional neural network. In the first step, a nonlinear transformation using polynomial function was applied in order to increase the dimension and better exploit correlations between features. For the number of features N, and the polynomial of degree d, the dimension M of the new space was given by: $M=\frac{(N+d)!}{N!d!}-1$. The increased efficiency of event classification can be attributed to nonlinear mappings of feature space, surpassing the effectiveness of linear approaches. This

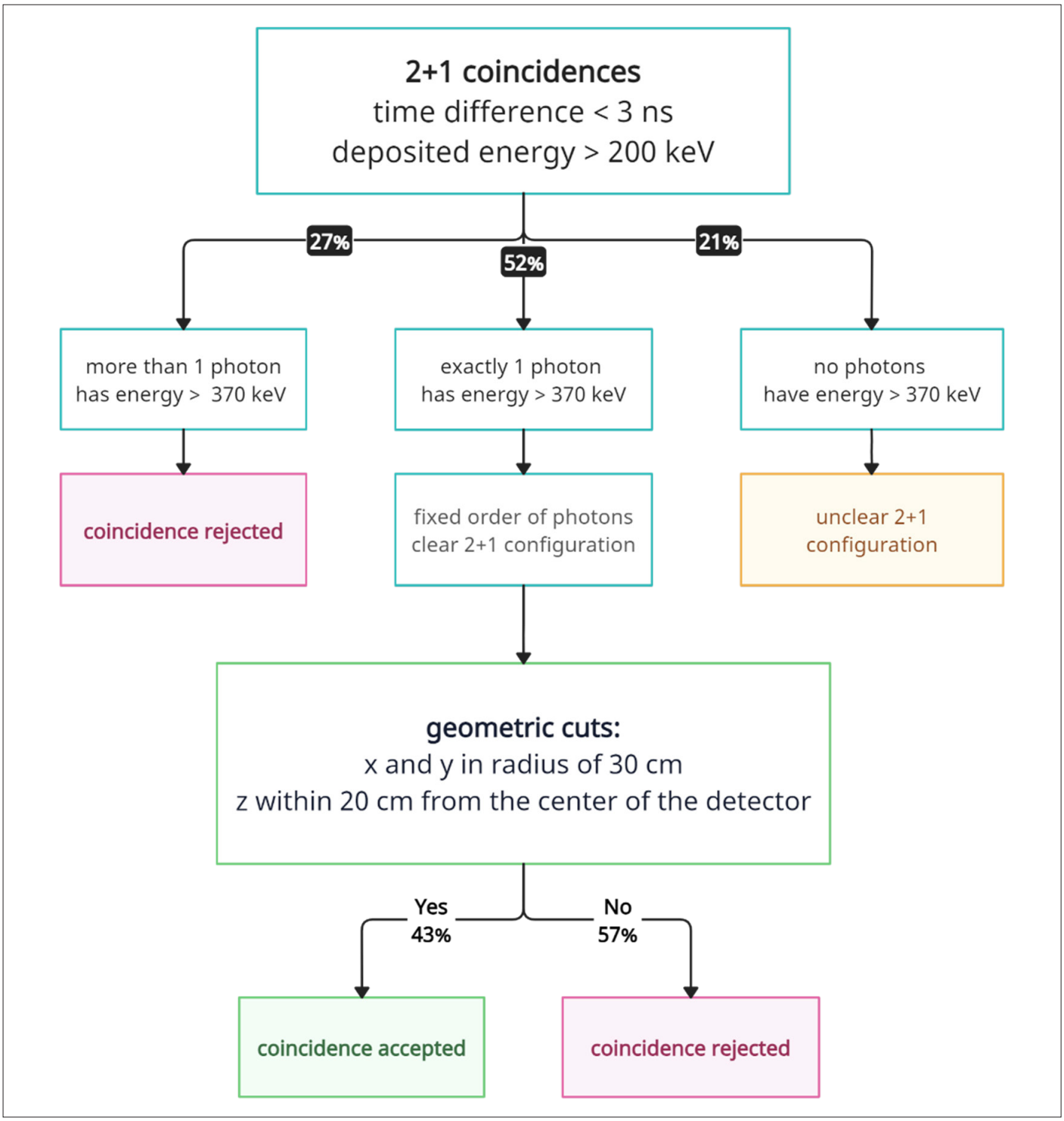

Fig. 1. Block diagram of the preprocessing methodology.

superiority is due to the enhanced feature space dimensional and improved utilization of feature correlations.

The image size of 30 × 30 pixels was selected for the following experiments. An analysis was conducted concerning the selection of the polynomial degree applied during the preprocessing stage. Feature overlapping (FO) and explained information (EI) served as metrics to guide this selection process [7]. The FO quantifies the proportion of features that jointly influence a single pixel in the resulting image. When no overlapping occurs each feature maps to a distinct pixel, resulting in an FO equal to 0. The EI parameter measures the percentage of variance in a dataset that can be attributed to the influence of the first two most significant eigenvectors. It provides insight into how well these eigenvectors

Tab. I. FO and EI vs. the degree of the polynomial.

DEGREE	NO. FEATURES	NO. NONZERO PIXELS	FO	EI
1	10	10	0%	84.4%
2	65	57	12%	85.1%
3	285	207	27%	85.2%
4	1000	441	56%	85.2%

capture and account for the variability present in the data. The results are presented in Tab. I.

The function with a third polynomial degree was chosen for subsequent analysis; the explained information was found to be equal to the maximum value (EI = 85.2%), and the feature overlapping (FO) was observed to be at 27%, lower than for a polynomial degree of 4.

Precision and recall represent critical metrics in the evaluation of classification models. Precision, also known as positive prediction value, quantifies the model's accuracy in recognizing positive instances, with a focus on minimizing the occurrence of false positives. Recall, also known as sensitivity and true positive rate, quantifies the proportion of actual positive instances correctly identified by a classification model among the total positive instances in the dataset (Fig. 2.).

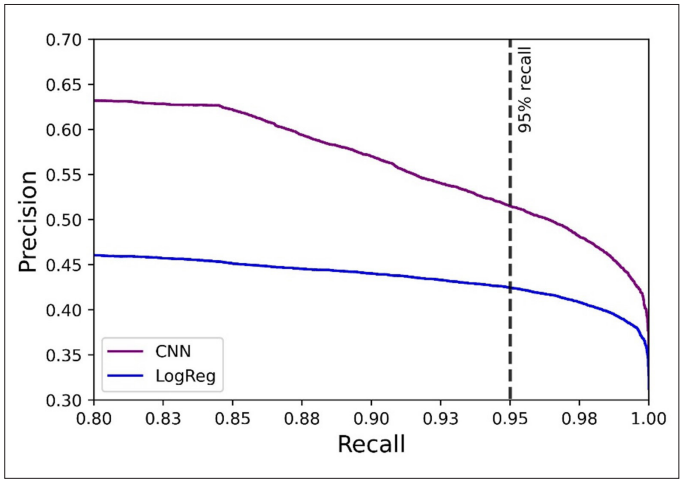

Fig. 2. Comparison of precision-recall curves for CNN and logistic regression classification models.

The precision for the CNN model, i.e. the percentage of correctly-classified coincidences (purple curve) attains a value of approximately 52% at a sensitivity of 95%, while the logistic regression model (blue curve) exhibits a precision of approximately 42%, signifying a notable distinction in classification accuracy between the two models. It is noteworthy that the input data predominantly comprised a signal accounting for only 31% (precision value for recall equals 100%). Consequently, this signifies that the developed method has increased the classification effectiveness by 68% (21%/31%). It is essential to consider that if the developed method is intended to complement positronium imaging [5], the feature set should exclude the positronium lifetime, as this characteristic should be estimated.

ACKNOWLEDGEMENTS

The contribution of Paweł Konieczka was done within the framework of the National Centre for Research and Development Project, No. POWR.03.02.00-00-I009/17 (Radiopharmaceuticals for molecularly targeted diagnosis and therapy, RadFarm. Operational Project Knowledge Education Development 2014–2020, co-financed by the European Social Fund).

REFERENCES

1. Badawi RD, Shi H, Hu P, Chen S, Xu T, Price PM, et al. First Human Imaging Studies with the EXPLORER Total-Body PET Scanner. J. Nucl. Med. 2018;60:299-303.
2. Holy EN, Fan AP, Alfaro ER, Fletcher E, Spencer BA, Cherry SR, et al. Non-invasive quantification and SUVR validation of [18F]-florbetaben with total-body EXPLORER PET. Alzheimer's Dement. 2022;18:e066123.
3. Jean JY, Mallon PE, Schrader DM. Introduction to Positron and Positronium Chemistry. In: Jean JY, Mallon PE, Schrader DM, editors. Principles and applications of positron and positronium chemistry. Singapore: World Scientific Publishing Co Pte Ltd; 2003. p. 1-15.
4. Moskal P. Positronium Imaging. In: 2019 IEEE Nuclear Science Symposium and Medical Imaging Conference (NSS/MIC). IEEE 2020; 2020; New York City. USA: 2020. p. 1-3.
5. Moskal P, Dulski K, Chug N, Curceanu C, Czerwiński E, Dadgar M, et al.: Positronium imaging with the novel multiphoton PET scanner. Sci. Adv. 2021;7:eabh4394.
6. Sharma A, Vans E, Shigemizu D, Boroevich KA, Tsunoda T. Deepinsight: A methodology to transform a non-image data to an image for convolution neural network architecture. Sci. Rep. 2019;9:11399.
7. Konieczka P, Raczyński L, Wiślicki W, Fedoruk O, Klimaszewski K, Kopka P, et al.: Transformation of PET raw data into images for event classification using convolutional neural networks. Math. Biosci. Eng. 2023;20:14938-58.
8. Moskal P, Niedźwiecki S, Bednarski T, Czerwiński E, Kapłon Ł, Kubicz E, et al. Test of a single module of the J-PET scanner based on plastic scintillators. Nucl. Instrum. Meth. Phys. Res. A. 2014;764:317-21.

9. Raczyński L, Moskal P, Kowalski P, Wiślicki W, Bednarski T, Białas P, et al. Compressive sensing of signals generated in plastic scintillators in a novel J-PET instrument. Nucl. Instrum. Meth. Phys. Res. A. 2015;786:105-12.

10. Moskal P, Rundel O, Alfs D, Bednarski T, Białas P, Czerwiński E, et al. Time resolution of the plastic scintillator strips with matrix photomultiplier readout for J-PET tomograph. Phys. Med. Biol. 2016;61:2025-47.

11. Niedźwiecki S, Białas P, Curceanu C, Czerwiński E, Dulski K, Gajos A, et al. J-PET: A New Technology for the Whole-body PET Imaging. Acta Phys. Polon. B. 2017;48:1567-76.

12. Jan S, Santin G, Strul D, Staelens S, Assie K, Autret D, et al. GATE: a simulation toolkit for PET and SPECT. Phys. Med. Biol. 2004;49:4543-62.

13. Sarrut D, Bała M, Bardiès M, Bert J, Chauvin M, Chatzipapas K, et al. Advanced Monte Carlo simulations of emission tomography imaging systems with GATE. Phys. Med. Biol. 2021;66:10TR03.

14. Dadgar M, Kowalski P. Gate simulation study of the 24-module J-PET scanner: Data analysis and image reconstruction. Acta Physica Polonica B. 2020;51:309-15.

15. Baran J, Krzemień W, Raczyński L, Bala M, Coussat A, Parzych S, et al. Realistic Total-Body J-PET Geometry Optimization – Monte Carlo Study. arXiv preprint. 2022;arXiv:2212.02285.

16. NEMA Standards Publication NU 2-2007: Performance measurements of Positron Emission Tomographs. Nat. Elect. Manuf. Assoc. Available from: https://psec.uchicago.edu/library/applications/PET/chien_min_NEMA_NU2_2007.pd.

17. Parzych S. Optimization of positronium imaging performance of simulated Modular J-PET scanner using GATE software. Symposium on new trends in nuclear and medical physics; 2023 Oct 18-20; Kraków. Poland; 2023.